Geophysical Research Letters

RESEARCH LETTER
10.1029/2023GL104373

The Role of the Pacific-Antarctic Ridge in Establishing the Northward Extent of Antarctic Sea-Ice

A. I. Ferola[1], Y. Cotroneo[1], P. Wadhams[2], G. Fusco[1], P. Falco[2], G. Budillon[1], and G. Aulicino[1]

[1]Department of Science and Technology, University of Napoli Parthenope, Napoli, Italy, [2]Department of Life and Environmental Sciences, Marche Polytechnic University, Ancona, Italy

Key Points:

- The Pacific-Antarctic Ridge diverts warm and cold core eddies northward, encouraging an expansion of Antarctic sea-ice at 150°W
- The Southern Ocean is characterized by the recurring formation of a sea-ice protrusion that extends to 60°S between 150°W and 140°W

Supporting Information:

Supporting Information may be found in the online version of this article.

Correspondence to:

Y. Cotroneo and G. Aulicino,
yuri.cotroneo@uniparthenope.it;
giuseppe.aulicino@uniparthenope.it

Citation:

Ferola, A. I., Cotroneo, Y., Wadhams, P., Fusco, G., Falco, P., Budillon, G., & Aulicino, G. (2023). The role of the Pacific-Antarctic Ridge in establishing the northward extent of Antarctic sea-ice. *Geophysical Research Letters*, *50*, e2023GL104373. https://doi.org/10.1029/2023GL104373

Received 1 MAY 2023
Accepted 8 MAY 2023

Abstract Monitoring the Antarctic sea-ice is essential for improving our knowledge of the Southern Ocean. We used satellite sea-ice concentration data for the 2002–2020 period to retrieve the sea-ice extent (SIE) and analyze its variability in the Pacific sector of the Southern Ocean. Results provide observational evidence of the recurring formation of a sea-ice protrusion that extends to 60°S at 150°W during the winter season. Furthermore, we discuss how the Pacific-Antarctic Ridge (PAR) influences this phenomenon. Our findings show that the northward deflection of the southern Antarctic Circumpolar Current front is driven by the PAR and is associated with the enhanced sea-ice advance. The PAR also constrains eddy trajectories, limiting their interaction with the sea-ice edge. These factors, within the 160°W–135°W sector, cause an average SIE increase of 61,000 km^2 and 46,293 km^2 per year more than the upstream and downstream areas, respectively.

Plain Language Summary Monitoring the variability of marine and continental ice is essential for the study of climate change. The aim of this study is to investigate the processes that favor the formation or melting of sea-ice in the Pacific sector of the Southern Ocean. To this end, we analyzed sea-ice variability over the last two decades (2002–2020) and its interaction with the Antarctic Circumpolar Current (ACC) and the Pacific-Antarctic Ridge (PAR), a topographic submarine feature that separates the Pacific and Antarctic plates. We used satellite data obtained through passive microwave sensors and altimetry for sea-ice and ACC eddy analysis, respectively. Our results provide observational evidence of the periodic formation of a sea-ice protrusion in the study area and show that the median extent of the sea-ice faithfully follows the PAR. Moreover, our results show that the PAR acts as a barrier that deflects the ACC and its associated eddies northward, which limits their ability to melt the sea-ice east of the PAR. These processes encourage the exceptional growth of the sea-ice in this area. These outcomes have strong implications for our understanding of sea-ice variability over the Southern Ocean.

1. Introduction

The accelerating rate of climate change is one of the main challenges humanity faces in the coming decades (IPCC, 2021). However, variations in the rates of change make it difficult to develop mitigation or adaptation strategies. Ice albedo feedback is a fundamental element of the global climate because it is responsible for the rapid oscillation between glacial and interglacial stages (Hall, 2004; Marcianesi et al., 2021). Sea-ice variability also affects freshwater fluxes that impact overturning circulation (Liu et al., 2022; Meccia et al., 2022; Wu et al., 2021), as well as biological processes and polar food webs (Castellani et al., 2020; Massom & Stammerjohn, 2010). Therefore, the study and monitoring of the variability in Antarctic Sea-ice concentration (SIC) and extent (SIE) is crucial for understanding and forecasting future of changes to Earth's climate (Parkinson, 2004).

The Southern Ocean (SO) can be characterized by large variations in SIC and SIE at both local and regional scales. For example, observations of the Bellingshausen Sea (in the Pacific sector of the SO) show strong decrease during the last four decades (Parkinson & Cavalieri, 2012; Stammerjohn et al., 2012; Wachter et al., 2021). However, the opposite occurred in the Ross Sea, where a slight increase in SIC and SIE was observed (Aulicino et al., 2014; Comiso et al., 2017; Parkinson, 2019). On a circumpolar basis, after exhibiting an upward trend since 1979, sea-ice shifted from record high to record low extents in 2016 (Parkinson, 2019). This unexpected decline underscored the incomplete understanding of the processes that influence Antarctic sea-ice distributions, including local and remote forcing mechanisms (Kennicutt et al., 2019; Meehl et al., 2019).

The main driving force behind the observed spatio-temporal changes in Antarctic SIE is usually related to the combination of atmospheric and oceanic phenomena (e.g., winds and SSTs; Blanchard-Wrigglesworth et al., 2021). A primary role is played by decadal-scale variability in oceanic and atmospheric circulation in the Southern Hemisphere (Cerrone, Fusco, Cotroneo et al., 2017; Cerrone, Fusco, Simmonds et al., 2017; Cerrone & Fusco, 2018; Cohen et al., 2013; Fogt & Bromwich, 2006; Fogt et al., 2012; Fusco et al., 2018; Meehl et al., 2019; Schlosser et al., 2018; Wang et al., 2021). Less is known about how sea-ice variability is affected by the Antarctic Circumpolar Current (ACC) (Nghiem et al., 2016), the track of mesoscale eddies (Ansorge et al., 2015), overturning cells (Kennicutt et al., 2019), and polynyas development (Campbell et al., 2019).

The ACC is the only zonally unlimited ocean current, and it is the primary means by which water, heat and salt are transferred between different ocean basins (Rintoul, 2018). Its flow is usually affected by the overlying westerlies. However, it has been demonstrated that wind impact on the ACC transport is significantly modulated by the bathymetry and the eddy presence (e.g., Bishop et al., 2016; de Boer et al., 2022). In fact, ACC has an equivalent barotropic vertical structure with an e-folding vertical scale of about 1,000 m (Killworth & Hughes, 2002). This means that, along the circumpolar path, its surface flow is strongly forced by interactions with the seafloor and submerged ridges shallower than roughly 3-km depth (Masich et al., 2015; Trani et al., 2011). De Boer et al. (2022) also showed that when the topographic barriers are removed the meridional variability in the wind stress curl contours generally disappears, and that the removal of Southern Hemisphere orography is also inconsequential to the wave-3 pattern. Additionally, Blanchard-Wrigglesworth et al. (2021) showed that mean meridional winds are much weaker than zonal winds over the Southern Ocean, with a reduced impact on ACC flow and associated eddies.

On the other hand, previous studies based on satellite and drifter data (e.g., Sokolov & Rintoul, 2009b and references therein) demonstrated that bathymetry plays indeed an important role in triggering the spawning of eddies from the ACC. When the mean flow encounters the major topography, it is forced to move equatorward/poleward, creating meanders that originate eddies (Barthel et al., 2017; Cai et al., 2022; Rintoul, 2018; Shi et al., 2023). Mesoscale eddies are ubiquitous in the Southern Ocean (Naveira Garabato et al., 2011) and affect the dynamic balance of the ACC (Rintoul, 2018), momentum exchange (Trani et al., 2014) and meridional heat transport (Cotroneo et al., 2013; Menna et al., 2020). Several eddy kinetic energy (EKE) hotspots are collocated with major topographic features distributed along the ACC path, such as the Pacific-Antarctic Ridge (PAR); the Kerguelen Plateau; the southwestern Indian Ridge; the Macquarie Ridge (south of the Tasman Sea) and the Campbell Plateau (Dufour et al., 2015; Falco & Zambianchi, 2011; Llort et al., 2018; Thompson & Sallée, 2012; Trani et al., 2014). However, model experiments showed that the EKE generally depends on the characteristics of the local topography, and the baroclinicity of the ACC flow, but it is not very sensitive to the variability of wind stress (Barthel et al., 2017; Cai et al., 2022; Shi et al., 2023).

In this study, we analyzed SIC data acquired around the Antarctic continent from May to December during the 2002–2020 period to determine SIEs and identify the general SIE behavior and regional variations. Then, we focused on the Pacific sector of the SO and the sea-ice protrusion east of the PAR (at approximately 150°W) that usually extends up to 60°S. The PAR is a divergent tectonic plate boundary located on the seafloor extending from approximately 56°S to Antarctica that separates the Pacific and Antarctic plates (Figure 2) and represents an important hot spot of EKE (Falco & Zambianchi, 2011). The observed sea-ice protrusion has been previously linked to atmospheric factors, such as the Amundsen Sea Low (e.g., Fogt and Scambos, 2013, 2014; Fogt and Stammerjohn, 2015; Scambos and Stammerjohn, 2018, 2019; Stammerjohn, 2016; Stammerjohn and Scambos, 2017; Turner et al., 2009, 2016), the Southern Annular Mode (e.g., Marshall, 2003; Son et al., 2010) and the katabatic wind regimes (e.g., Farooq et al., 2023) that can explain part of its seasonal and interannual variability. Conversely, few studies have analyzed if/how local bathymetry exerts a control on this protrusion and what allows its recurrent formation, besides the seasonal and interannual variability driven by oceanic and atmospheric forcing (Nghiem et al., 2016).

Here, we confirm from observed data that the PAR influences the persistence of the sea-ice cover in this sector of the SO (Roach & Speer, 2019), guiding the ACC mean flow, constraining the location of its fronts and acting as a barrier to eddies that should guarantee the zonal heat transport when the ACC is deflected northward. To achieve this, the ACC front position, mesoscale eddy trajectories and their distribution were analyzed. Datasets and methodologies are described in Section 2. Section 3 reports and discusses the results. Conclusions are summarized in Section 4.

2. Data and Methods

2.1. Sea-Ice Concentration and Extent

In this study we used daily 3.5 km resolution SIC data (Spreen et al., 2008) for May to December between 2002 and 2020. This data is distributed by the University of Bremen (https://seaice.uni-bremen.de). These observations were collected through microwave passive sensors, including the Advanced Microwave Scanning Radiometer—Earth Observing System sensor (AMSR-E) mounted on the Aqua satellite and the Advanced Microwave Scanning Radiometer 2 (AMSR 2) mounted on the GCOM-W1 satellite. Monthly SIC maps (May to December) covering the SO and its Pacific sector (80°W–160°E) during the 2002–2020 interval were obtained, taking into account the absence of data during November and December 2011 and in May 2012. From this data set, we extracted the SIE (namely, the northernmost edge of the ice-covered ocean areas where SIC is greater than 15%) and computed the median value (0%–90%) to describe the boundary position of the sea-ice for each month analyzed, as also described in Ansorge et al. (2015).

2.2. Mesoscale Eddy Trajectories

In this study we use eddy trajectories and properties (e.g., translational mean speed and lifetime) from the META3.1 DT allsat data set (Pegliasco et al., 2022). This data set was published by AVISO (https://www.aviso.altimetry.fr/en/data/products/value-added-products/global-mesoscale-eddytrajectory-product/meta3-1-exp-dt.html) and was generated using the methodology outlined in Mason et al. (2014) and the DUACS DT2018 (Taburet et al., 2019) gridded 0.25° sea surface height data. The DUACS Sea Level product (published by the Copernicus Climate Change Service) is a daily time series of gridded Sea Surface Height (SSH), that began in January 1993 and is still being updated. We used this data set to statistically describe the eddies in the study area, produce warm and cold core eddy distribution maps over the SO during the study period (2002–2020), and investigate eddy dynamics in relation to the ocean bathymetry, the ACC fronts position and the SIE variability.

3. Results and Discussion

The maps of the SO SIC were averaged over the 2002–2020 period for each month from May to December and revealed the existence of two interesting areas in the Indian and Pacific sectors of the SO (Figure 1).

The first is represented by a recurring sea-ice deflection (at approximately 30°E) that is linked to the southward path of mesoscale eddies in this area (Ansorge et al., 2015) and to the presence of the South-West Indian Ridge, which significantly influences the sea-ice dynamics in that region.

The second one can be identified in the Pacific sector, where a recurring, and enhanced, sea-ice advance is located at approximately 150°W. At this longitude the sea-ice extends northward to approximately 60°S, and represents an interesting regional behavior that determines the northward shift of the Marginal Ice Zone (MIZ). The recurring SIE maximum is clearly evident during the peak winter months (i.e., August and September), with some annual variability, as previously observed by Parkinson (2019).

The presence of the sea-ice protuberance in the longitude band between 150°W and 140°W is clearer in the maps of the median SIE presented in Figure 2a. The contour lines of the median SIE corresponding to the western side of the protuberance are aligned along the main SW-NE axis of the PAR. At approximately 150°W, the PAR extends to lower latitudes shifting from approximately 66°S at 180°–60°S at 150°W; thus, the maximum SIE can be identified immediately further east of the PAR during most of the analyzed months. These characteristics are more evident during the winter sea-ice growth phase in July and August, and the northern edge of the protuberance shifts progressively further east due to the forcing of the ACC and wind during the following months (e.g., from September to December). This eastward migration is also encouraged by the ACC incidence on the sea-ice protuberance, which may be greater in the period in which the ice is not as thick.

This behavior is likely connected to the northward shift of ACC streamlines and fronts (including the southern ACC front—sACCf) due to the presence of the PAR (Figure 2b). Starting from the west, the ACC initially follows the PAR, and is diverted to the north. However, when it reaches 150°W, it crosses the PAR at the Udintsev and Eltanin fracture zones, which are areas of enhanced EKE development. This result agrees with the literature, which states that flow instabilities, most notably the baroclinic or shear flow instability mechanism (Best

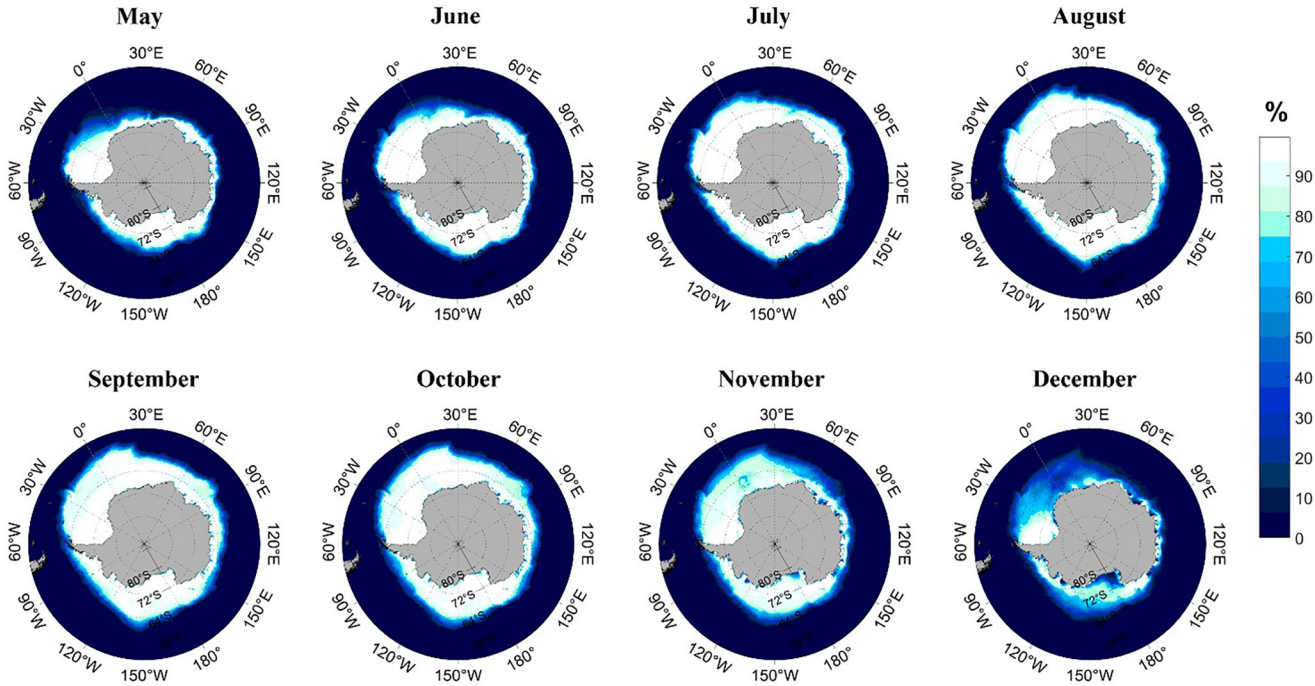

Figure 1. Sea-ice concentration averaged over the 2002–2020 period for the months from May to December. The concentration is expressed as a percentage (shown in color).

et al., 1999; Wolff, 1999), and the consequent eddy generation sites are known to be closely correlated with areas where the ACC crosses prominent bottom topographic features, such as mid-ocean ridges (Cotroneo et al., 2013; Shi et al., 2023; Sokolov & Rintoul, 2009a; Swart et al., 2008; Trani et al., 2014).

Similarly, we propose that the PAR also influences the path of ACC eddies that extend deeper into the water column and affect their interaction with sea-ice in the study area (Roach & Speer, 2019). The sea level anomaly (SLA) derived eddy trajectories provided by DUACS were processed to generate monthly anticyclonic (warm core) and cyclonic (cold core) eddy distribution maps over the Pacific sector of the SO from May to December during the 2002–2020 period. To evaluate the relationships between eddies and sea-ice, we superimposed the median SIE contours for each month on the monthly eddy distribution map (see Figure 3 and Figure S1 in Supporting Information S1).

In both August and December, the concentration of eddies on the eastern side (downstream) of the PAR is much lower than that on the western side (upstream). This is explained by the presence of shallower depths that influence both the formation and propagation of the vortices. Previous studies have reported that eddies do not reach areas shallower than 2,000 m (Cotroneo et al., 2013) because of the deep structure of eddies and the conservation of potential vorticity (Fu et al., 2010; Lu & Speer, 2010; Sallée et al., 2011; Thompson & Sallée, 2012).

The cyclonic eddies (green trajectories in Figure 3) follow the PAR, as well as the contours of the median ice extent. They are characterized by longer and more uniform trajectories in contrast to the anticyclonic eddies (in red), which appear less regularly and present fragmented trajectories. Some eddies also seem to cross the median SIE while following the Ross Gyre circulation (Figure 3). As satellites (altimetry) cannot provide SSH data below ice, we infer that the presence of these eddies is due to the difference between the represented median SIE monthly average (2002–2020) and the actual SIE during a specific month/year. The ice-free areas immediately east of the PAR are indeed characterized by a very low number of eddies. Furthermore, a predominance of cold core eddies along the northern sea-ice boundary can be observed.

We integrated these qualitative results with a statistical analysis providing quantitative information about the main characteristics of the mapped mesoscale eddies. Warm and cold core eddies identified during the 2002–2019 period in the area south of 45°S between 120°E and 120°W were analyzed via the observations of their mean characteristics and associated standard deviations. Since the ACC constantly flows eastward, this subset

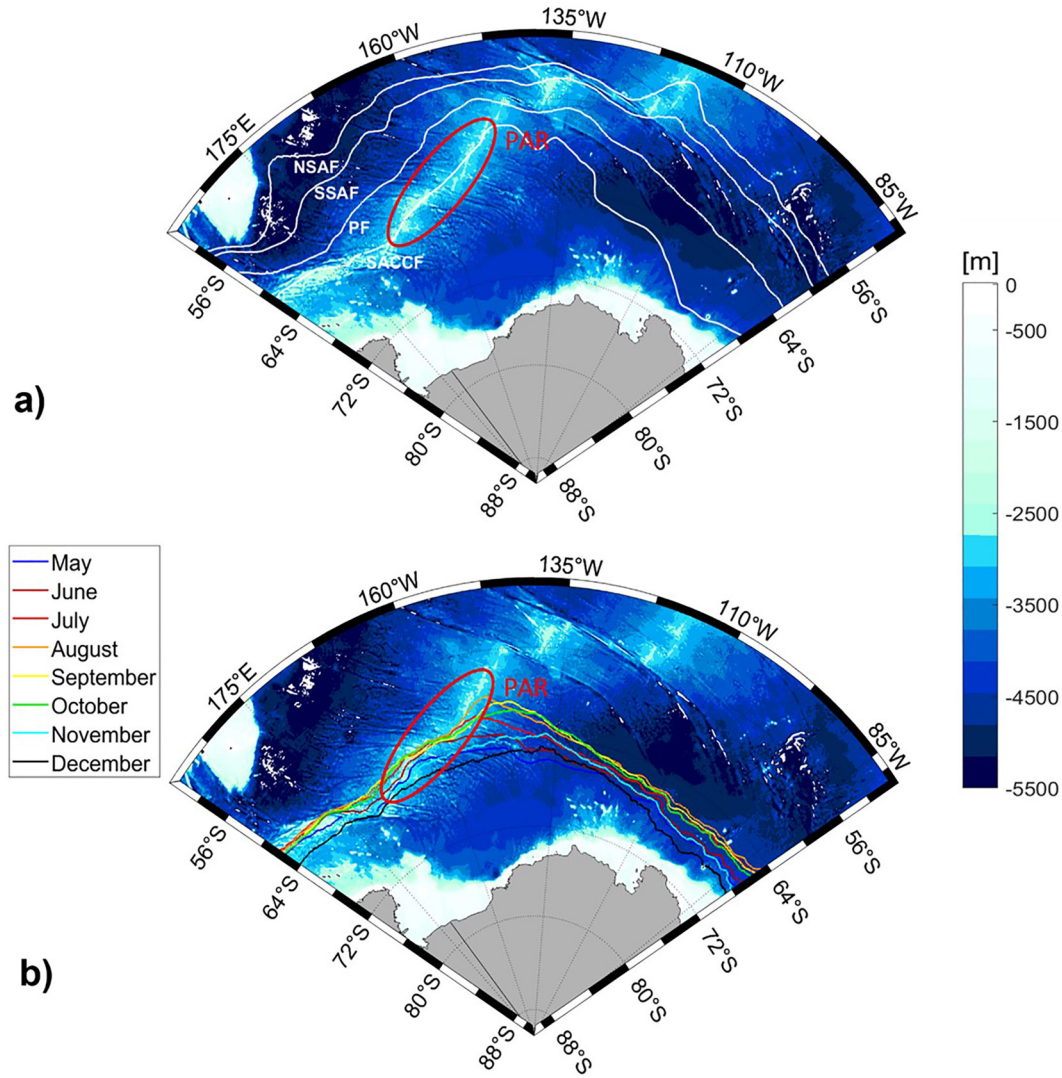

Figure 2. (a) Mean positions of the main Antarctic Circumpolar Current fronts (white lines), adapted from Menna et al. (2020). From north to south: Northern Sub-Antarctic Front (NSAF), Southern Sub-Antarctic Front (SSAF), Polar front (PF) and Southern ACC Front (sACCf) as defined by Orsi et al. (1995) and Sallée et al. (2008). (b) Median sea-ice extent (0%–90% sea-ice concentration) for the months between May and December (colorcoded), obtained through SIC data over the 2002–2020 period. The bathymetry of the Pacific sector of the Southern Ocean is represented and expressed in meter. The position of the Pacific-Antarctic Ridge (PAR) is circled in red.

includes the mesoscale structures located west of the PAR (i.e., upstream of the ridge) which are the most interesting for studying their interaction with the sea-ice protuberance.

The overall number of cyclonic and anticyclonic eddies is very similar, as well as the respective average characteristics, such as diameter, lifetime, Δ SSH (i.e., the difference in SSH between the center and the SSH around the contour that defines the edge of the vortex), rotational and translational speed (see Table S1 in Supporting Information S1). The data used to evaluate the eddies' physical parameters are direct measurements obtained through remote sensing, apart from the translational speed which was derived by analyzing the distance between two consecutive positions of the same eddy. These statistics, and the eddies' tracks, confirm that both cyclonic and anticyclonic structures have similar opportunities to reach and interact with the sea-ice edge if they form in the same area.

To examine where anticyclonic eddies were concentrated, we produced frequency maps for 1993–2020 using a 0.5° × 0.5° grid (Figure 4). Each 0.5 × 0.5° cell contains the number of eddies that passed through that cell

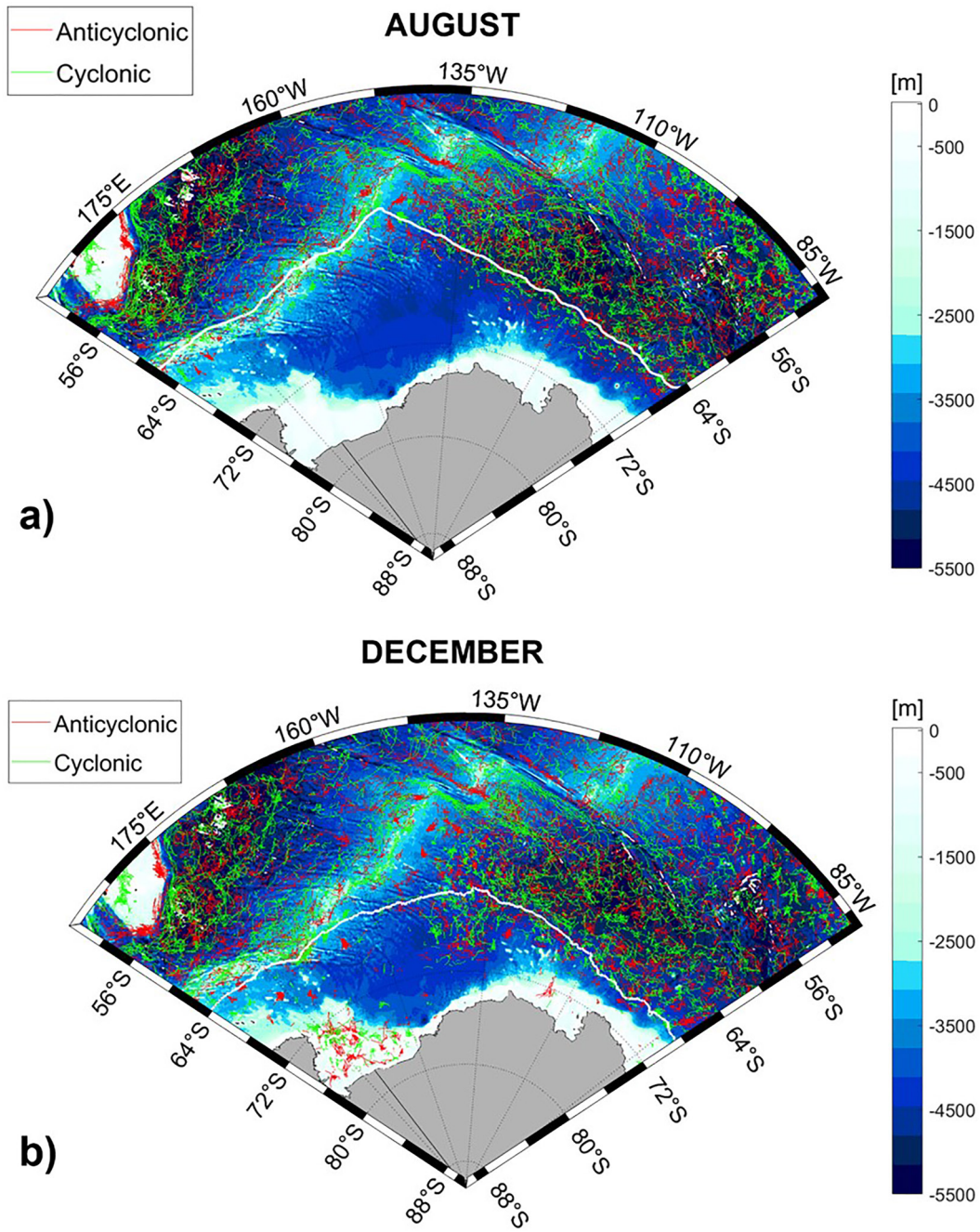

Figure 3. (a) August and (b) December anticyclonic (red) and cyclonic (green) eddy distribution maps overlapped on the respective median ice extent (0%–90%), relative to the 2002–2020 period. The bathymetry is expressed in meters (see color bar).

just once, which excludes the eddies recirculating within the same grid cell. Figure 4a shows that the western (upstream) side of the PAR (identified by the 2,500 and 2,600 m depth isolines) is characterized by a higher concentration of eddies than the eastern (downstream) side.

Conversely, an increase in the number of eddies is observed downstream of the PAR (56°S and 135°W), next to the Udintsev fracture zone, where the ACC and the eddies overcame the influence of the PAR. Furthermore, it is interesting to note that when comparing anticyclonic (Figure 4b) and cyclonic (Figure 4c) eddy frequency maps, a larger number of cold core than warm core structures can be identified over the PAR.

10.1029/2023GL104373

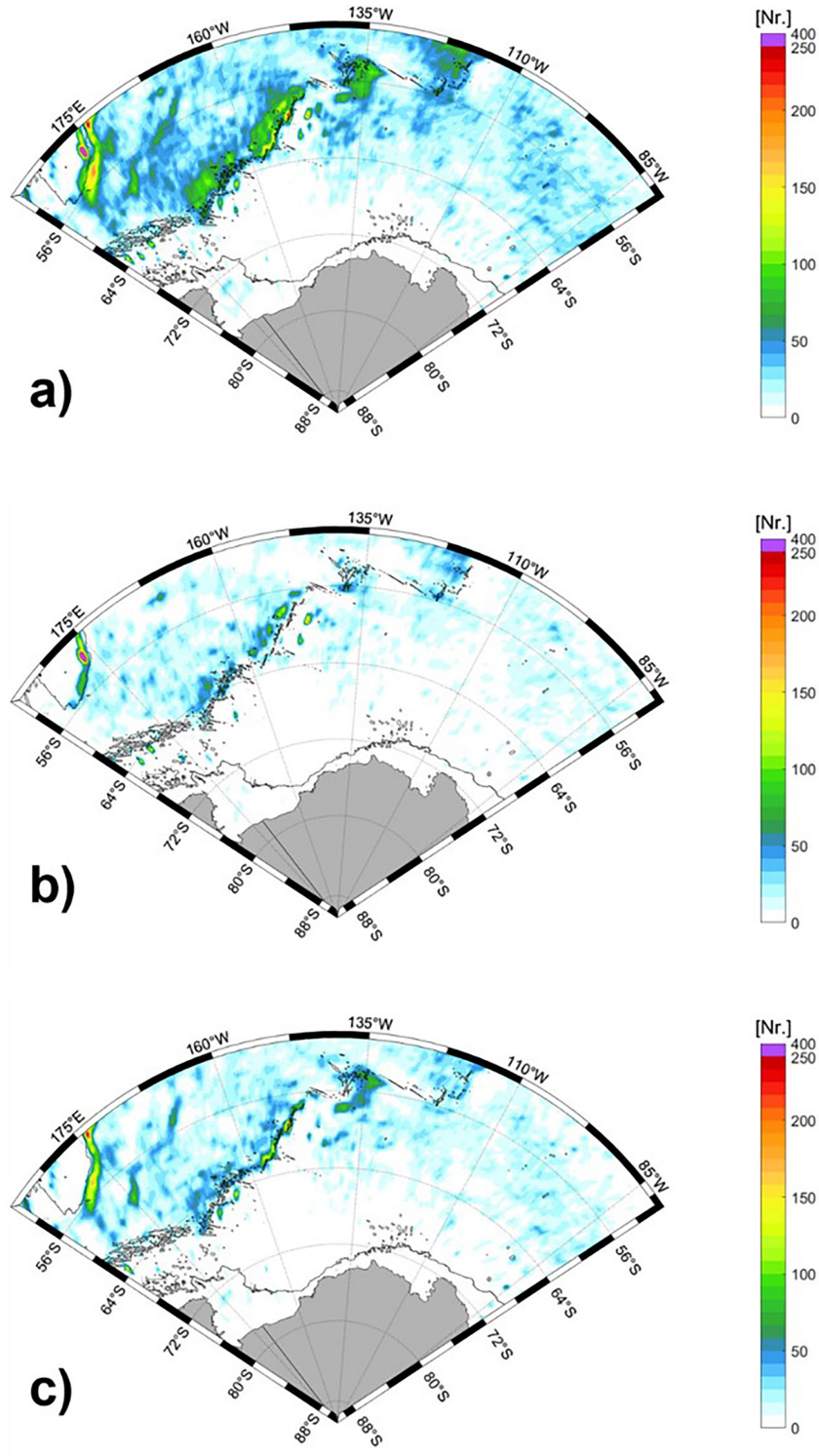

Figure 4. Frequency maps of (a) all the observed eddies and their classification in (b) anticyclonic and (c) cyclonic structures during the 1993–2020 period within 0.5 × 0.5° grid cells. The −2,500 and −2,600 m bathymetric contour lines are represented in black.

Therefore, as shown in both Figures 3 and 4, the concentration of eddies is much greater in the sectors immediately west of 150°W and east of 140°W, which aligns with the region where the PAR shifts more markedly toward lower latitudes (at approximately 150°W).

Thus, the SIE is influenced by this asymmetric distribution of the eddies. In fact, previous studies describing the mechanisms of interaction between cyclonic/anticyclonic eddies and the MIZ in the Northern Hemisphere (e.g., Manucharyan & Thompson, 2017) demonstrate that both cold core and warm core eddies favor sea-ice melting and MIZ retreat. However, in the study area, the presence of the PAR represents a strong barrier that prevents cold core eddies from propagating eastward (toward the MIZ) and forces them to move northward. By diverting eddy trajectories northward, the PAR strongly constrains the eddy patterns and prevents or reduces their interaction with the sea-ice edge that generally follows the PAR contours for all the months analyzed (Figure 2a). The PAR effect is also confirmed by the absence of eddies along the eastern (downstream) edge during the austral summer months, when SIE is limited to higher latitudes (Figure 3b). This favors the exceptional growth of the SIE at 150°W, which is disrupted only by sporadic anticyclonic mesoscale structures coming from the east of the ice protuberance. Owing to the absence of a ridge, the oceanic area east of the PAR (130°W–150°W) is instead characterized by a greater freedom of motion for eddies, which results in less regular median SIE contours due to eddies chaotic trajectories and their role in favoring sea-ice melting.

In summary, the PAR acts as a shield sustaining the formation of sea-ice by diverting the ACC northward (Figure 2b) and allowing cold water masses to reach more northerly locations. The PAR also influences the meridional heat transport by deflecting the eddy tracks in the area and preventing their interaction with the MIZ. This action favors the formation of the observed recurring sea-ice protuberance at approximately 150°W that results in an exceptional growth of the ice-covered area in this sector.

To provide a quantitative estimation of this phenomenon, we divided the Pacific sector of the SO into three longitudinal bands, each 25° wide (i.e., 175°E–160°W, 160°W–135°W and 135°W–110°W), and calculated the ice area that forms between May and August in each sector based on the latitudinal difference between the respective median SIE contours over the study period. As expected, the sector that includes the PAR (i.e., 160°W–135°W) is characterized by an expansion in sea-ice (104,537 km^2) that is approximately twice that observed in the neighboring western (43,720 km^2) and eastern (58,244 km^2) sectors.

4. Conclusions

In this study, we explored May to December sea-ice variability around the Antarctic continent over the 2002–2020 period. This analysis allowed us to identify and describe the recurring sea-ice protuberance that forms in the Pacific sector of the SO, extending equatorward to 60°S at approximately 150°W longitude. This structure is usually identified immediately east of the PAR, a divergent tectonic plate that is significantly shallower than the surrounding ocean. To this end, we processed available altimetric information to generate frequency and distribution maps of the trajectories of the mesoscale cyclonic and anticyclonic eddies in the study area during the last two decades. Then, we carried out a combined analysis involving collocated observations of sea-ice and SSH, which confirmed that the PAR acts as a barrier that deflects the flow of ACC to the north; therefore, most of the eddies that reach the PAR approach from the western side. This action has an impact on the local SIE variability, allowing cold water masses to reach lower latitudes, reducing the interaction of eddies and the ACC with the sea-ice edge, and favor the formation of the sea-ice protuberance observed just east of the PAR. This results in an expansion of the ice-covered area between 160°W and 135°W, which includes the PAR. The SIE in this region surpasses the adjacent upstream and downstream sectors by approximately 60,817 and 46,293 km^2, respectively.

Based on these results, it would be interesting to broaden the period of analyses to at least 30 years in order to properly analyze climatological impacts. It may be possible to extend the record of eddy tracks back to 1993, the first year in which reliable satellite altimetry is available. Unfortunately, the AMSR-E and AMSR2 products do not allow us to obtain information prior to 2002. Therefore, analyses prior to the past twenty years require the use of different sea-ice products with much lower spatial resolutions (e.g., the Special Sensor Microwave Imager and the Special Sensor Microwave Imager/Sounder which were carried onboard the Defense Meteorological Satellite Program satellites since 1987). However, to ensure homogeneity using SIC—SIE products characterized by different nominal resolutions, a comparison of respective results obtained during coincident periods would be desirable.

Future work will also focus on meteorological parameters, for instance, to investigate the relationship between the PAR, sea-ice and local synoptic winds, to determine whether there are wind patterns that are favorable to SIE increases and, if so, which patterns contribute to regional sea-ice protrusion formation, besides the known seasonal and interannual variability driven by atmospheric forcing.

Data Availability Statement

All observational datasets used in this study are publicly available. Sea-ice products analyzed in this study are available from the University of Bremen at https://seaice.uni-bremen.de/data/amsre/asi_daygrid_swath/s3125/ and https://seaice.uni-bremen.de/data/amsr2/asi_daygrid_swath/s3125/. The META3.1exp delayed time dataset is available from AVISO+ at https://www.aviso.altimetry.fr/en/data/products/value-added-products/global-mesoscale-eddy-trajectory-product/meta3-1-exp-dt.html.

Acknowledgments
This work was undertaken within the framework of the PON R&I 2014–2020 "AIM—Attraction and International Mobility" at Università degli Studi di Napoli Parthenope. It was carried out thanks to financial support from the Sea-ice—Wave Interaction Monitoring for Marginal Ice NaviGation (SWIMMING —Grant PNRA18_00298) and the Antarctic Circumpolar Current Eddies Survey and Simulations (ACCESS—Grant PNRA19_00032) projects of the Italian National Program for Research in Antarctica (PNRA). Additionally, we would like to thank Dr Christopher J. Roach, two additional anonymous referees and the academic editor for their helpful and careful comments.

References

Ansorge, I. J., Jackson, J. M., Reid, K., Durgadoo, J. V., Swart, S., & Eberenz, S. (2015). Evidence of a southward eddy corridor in the South -West Indian Ocean. *Deep Sea Research Part II: Topical Studies in Oceanography*, *119*, 69–76. https://doi.org/10.1016/j.dsr2.2014.05.012

Aulicino, G., Fusco, G., Kern, S., & Budillon, G. (2014). Estimation of sea-ice thickness in Ross and Weddell seas from SSM/I brightness temperatures. *IEEE Transactions on Geoscience and Remote Sensing*, *52*(7), 4122–4140. https://doi.org/10.1109/TGRS.2013.2279799

Barthel, A., Hogg, A. M. C., Waterman, S., & Keating, S. (2017). Jet–topography interactions affect energy pathways to the deep southern Ocean. *Journal of Physical Oceanography*, *47*(7), 1799–1816. https://doi.org/10.1175/JPO-D-16-0220.1

Best, S. E., Ivchenko, V. O., Richards, K. J., Smith, R. D., & Malone, R. C. (1999). Eddies in numerical models of the Antarctic circumpolar current and their influence on the mean flow. *Journal of Physical Oceanography*, *29*(3), 328–350. https://doi.org/10.1175/1520-0485(1999)029<0328:EINMOT>2.0.CO;2

Bishop, S. P., Gent, P. R., Bryan, F. O., Thompson, A. F., Long, M. C., & Abernathey, R. (2016). Southern Ocean overturning compensation in an eddy-resolving climate simulation. *Journal of Physical Oceanography*, *46*(5), 1575–1592. https://doi.org/10.1175/JPOD-15-0177.1

Blanchard-Wrigglesworth, E., Roach, L. A., Donohoe, A., & Ding, Q. (2021). Impact of winds and Southern Ocean SSTs on Antarctic sea ice trends and variability. *Journal of Climate*, *34*(3), 949–965. https://doi.org/10.1175/JCLI-D-20-0386.1

Cai, Y., Chen, D., Mazloff, M. R., Lian, T., & Liu, X. (2022). Topographic modulation of the wind stress impact on eddy activity in the Southern Ocean. *Geophysical Research Letters*, *49*(13). https://doi.org/10.1029/2022GL097859

Campbell, E. C., Wilson, E. A., Moore, G. W. K., Riser, S. C., Brayton, C. E., Mazloff, M. R., & Talley, L. D. (2019). Antarctic offshore polynyas linked to Southern Hemisphere climate anomalies. *Nature*, *570*(7761), 319–325. https://doi.org/10.1038/s41586-019-1294-0

Castellani, G., Schaafsma, F. L., Arndt, S., Lange, B. A., Peeken, I., Ehrlich, J., et al. (2020). Large-scale variability of physical and biological sea-ice properties in polar oceans. *Frontiers in Marine Science*, *7*, 536. https://doi.org/10.3389/fmars.2020.00536

Cerrone, D., & Fusco, G. (2018). Low-frequency climate modes and Antarctic sea ice variations, 1982-2013. *Journal of Climate*, *31*(1), 147–175. https://doi.org/10.1175/JCLI-D-17-0184.1

Cerrone, D., Fusco, G., Cotroneo, Y., Simmonds, I., & Budillon, G. (2017). The Antarctic circumpolar wave: Its presence and interdecadal changes during the last 142 years. *Journal of Climate*, *30*(16), 6371–6389. https://doi.org/10.1175/JCLI-D-16-0646.1

Cerrone, D., Fusco, G., Simmonds, I., Aulicino, G., & Budillon, G. (2017). Dominant covarying climate signals in the southern ocean and Antarctic sea ice influence during the last three decades. *Journal of Climate*, *30*(8), 3055–3072. https://doi.org/10.1175/JCLI-D-16-0439.1

Cohen, L., Dean, S., & Renwick, J. (2013). Synoptic weather types for the Ross Sea region, Antarctica. *Journal of Climate*, *26*(2), 636–649. https://doi.org/10.1175/JCLI-D-11-00690.1

Comiso, J. C., Gersten, R. A., Stock, L. V., Turner, J., Perez, G. J., & Cho, K. (2017). Positive trend in the Antarctic sea ice cover and associated changes in surface temperature. *Journal of Climate*, *30*(6), 2251–2267. https://doi.org/10.1175/jcli-d-16-0408.1

Cotroneo, Y., Budillon, G., Fusco, G., & Spezie, G. (2013). Cold core eddies and fronts of the Antarctic circumpolar current south of New Zealand from in situ and satellite data. *Journal of Geophysical Research: Oceans*, *118*(5), 2653–2666. https://doi.org/10.1002/jgrc.20193

de Boer, A. M., Hutchinson, D. K., Roquet, F., Sime, L. C., Burls, N. J., & Heuzé, C. (2022). The impact of southern ocean topographic barriers on the ocean circulation and the overlying atmosphere. *Journal of Climate*, *35*(18), 5805–5821. https://doi.org/10.1175/JCLI-D-21-0896.1

Dufour, C. O., Griffies, S. M., de Souza, G. F., Frenger, I., Morrison, A. K., Palter, J. B., et al. (2015). Role of mesoscale eddies in cross-frontaltransport of heat and biogeochemical tracers in the Southern Ocean. *Journal of Physical Oceanography*, *45*(12), 3057–3081. https://doi.org/10.1175/JPO-D-14-0240.1

Falco, P., & Zambianchi, E. (2011). Near-surface structure of the Antarctic circumpolar current derived from world ocean circulation experiment drifter data. *Journal of Geophysical Research*, *116*(C5), C05003. https://doi.org/10.1029/2010JC006349

Farooq, U., Rack, W., McDonald, A., & Howell, S. (2023). Representation of sea ice regimes in the Western Ross Sea, Antarctica, based on satellite imagery and AMPS wind data. *Climate Dynamics*, *60*(1–2), 227–238. https://doi.org/10.1007/s00382-022-06319-9

Fogt, R. L., & Bromwich, D. H. (2006). Decadal variability of the ENSO teleconnection to the high-latitude south Pacific governed by coupling with the southern annular mode. *Journal of Climate*, *19*(6), 979–997. https://doi.org/10.1175/JCLI3671.1

Fogt, R. L. & Scambos, T. A. (Eds.) (2013). Antarctica. In *"State of the climate in 2012". Bulletin of the American Meteorological Society* (Vol. 94(8), pp. S133–S145).

Fogt, R. L. & Stammerjohn, S. (Eds.) (2015). Antarctica. In *"State of the climate in 2014". Bulletin of the American Meteorological Society* (Vol. 96(7), pp. S149–S165).

Fogt, R. L., Wovrosh, A. J., Langen, R. A., & Simmonds, I. (2012). The characteristic variability and connection to the underlying synoptic activity of the Amundsen-Bellingshausen Seas Low. *Journal of Geophysical Research*, *117*(D7), D07111. https://doi.org/10.1029/2011JD017337

Fogt, R. L. & Scambos, T. (Eds.) (2014). Antarctica. In *"state of the climate in 2013". Bulletin of the American Meteorological Society* (Vol. 95(7), pp. S143–S154).

Fu, L.-L., Chelton, D. B., Le Traon, P.-Y., & Morrow, R. (2010). Eddy dynamics from satellite altimetry. *Oceanography*, *23*(4), 1425–25. https://doi.org/10.5670/oceanog.2010.02

Fusco, G., Cotroneo, Y., & Aulicino, G. (2018). Different behaviours of the Ross and Weddell seas surface heat fluxes in the period 1972–2015. *Climate*, *6*(1), 17. https://doi.org/10.3390/cli6010017

Hall, A. (2004). The role of surface albedo feedback in climate. *Journal of Climate*, *17*(7), 1550–1568. https://doi.org/10.1175/1520-0442(2004)017%3C1550:TROSAF%3E2.0.CO;2

IPCC. (2021). In V. Masson-Delmotte, P. Zhai, A. Pirani, S. L. Connors, C. Péan, et al. (Eds.), *Climate change 2021: The physical science basis. Contribution of working Group I to the sixth assessment report of the intergovernmental panel on climate change*. Cambridge University Press.

Kennicutt, M. C., Bromwich, D., Liggett, D., Njåstad, B., Peck, L., Rintoul, S. R., et al. (2019). Sustained Antarctic research: A 21st century imperative. *One Earth*, *1*(1), 95–113. https://doi.org/10.1016/j.oneear.2019.08.014

Killworth, P. D., & Hughes, C. W. (2002). The Antarctic Circumpolar Current as a free equivalent-barotropic jet. *Journal of Marine Research*, *60*(1), 19–45. https://doi.org/10.1357/002224002762341230

Liu, F., Lu, J., Kwon, Y.-O., Frankignoul, C., & Luo, Y. (2022). Freshwater flux variability lengthens the period of the low-frequency AMOC variability. *Geophysical Research Letters*, *49*(20), e2022GL100136. https://doi.org/10.1029/2022GL100136

Llort, J., Langlais, C., Matear, R., Moreau, S., Lenton, A., & Strutton, P. G. (2018). Evaluating Southern Ocean carbon eddy-pump from biogeochemical-Argo floats. *Journal of Geophysical Research: Oceans*, *123*(2), 971–984. https://doi.org/10.1002/2017JC012861

Lu, J., & Speer, K. (2010). Topography, jets, and eddy mixing in the Southern Ocean. *Journal of Marine Research*, *68*(3–4), 479–502. https://doi.org/10.1357/002224010794657227

Manucharyan, G. E., & Thompson, A. F. (2017). Submesoscale sea ice-ocean interactions in marginal ice zones. *Journal of Geophysical Research: Oceans*, *122*(12), 9455–9475. https://doi.org/10.1002/2017JC012895

Marcianesi, F., Aulicino, G., & Wadhams, P. (2021). Arctic sea ice and snow cover albedo variability and trends during the last three decades. *Polar Science*, *28*, 100617. https://doi.org/10.1016/j.polar.2020.100617

Marshall, G. J. (2003). Trends in the southern annular mode from observations and reanalyses. *Journal of Climate*, *16*(24), 4134–4143. https://doi.org/10.1175/1520-0442(2003)016<4134:titsam>2.0.co;2

Masich, J., Chereskin, T. K., & Mazloff, M. R. (2015). Topographic form stress in the southern ocean state estimate. *Journal of Geophysical Research: Oceans*, *120*(12), 7919–7933. https://doi.org/10.1002/2015JC011143

Mason, E., Pascual, A., & McWilliams, J. C. (2014). A new sea surface height–based code for oceanic mesoscale eddy tracking. *Journal of Atmospheric and Oceanic Technology*, *31*(5), 1181–1188. https://doi.org/10.1175/JTECH-D-14-00019.1

Massom, R. A., & Stammerjohn, S. E. (2010). Antarctic sea ice change and variability – Physical and ecological implications. *Polar Science*, *4*(2), 149–186. https://doi.org/10.1016/j.polar.2010.05.001

Meccia, V. L., Fuentes-Franco, R., Davini, P., Bellomo, K., Fabiano, F., Yang, S., & von Hardenberg, J. (2022). Internal multi-centennial variability of the Atlantic meridional overturning circulation simulated by EC-Earth3. *Climate Dynamics*. https://doi.org/10.1007/s00382-022-06534-4

Meehl, G. A., Arblaster, J. M., Chung, C. T., Holland, M. M., DuVivier, A., Thompson, L., & Bitz, C. M. (2019). Sustained ocean changes contributed to sudden Antarctic sea ice retreat in late 2016. *Nature Communications*, *10*(1), 1–9. https://doi.org/10.1038/s41467-018-07865-9

Menna, M., Cotroneo, Y., Falco, P., Zambianchi, E., Lemma, R., Poulain, P., et al. (2020). Response of the Pacific sector of the southern ocean to wind stress variability from 1995 to 2017. *Journal of Geophysical Research: Oceans*, *125*(10), e2019JC015696. https://doi.org/10.1029/2019JC015696

Naveira Garabato, A. C., Ferrari, R., & Polzin, K. L. (2011). Eddy stirring in the Southern Ocean. *Journal of Geophysical Research*, *116*(C9), C09019. https://doi.org/10.1029/2010JC006818

Nghiem, S. V., Rigor, I. G., Clemente-Colón, P., Neumann, G., & Li, P. P. (2016). Geophysical constraints on the Antarctic sea ice cover. *Remote Sensing of Environment*, *181*, 281–292. https://doi.org/10.1016/j.rse.2016.04.005

Orsi, A. H., Whitworth, T., & Nowlin, W. D. (1995). On the meridional extent and fronts of the Antarctic circumpolar current. *Deep Sea Research Part I: Oceanographic Research Papers*, *42*(5), 641–673. https://doi.org/10.1016/0967-0637(95)00021-W

Parkinson, C. L. (2004). Southern Ocean sea ice and its wider linkages: Insights revealed from models and observations. *Antarctic Science*, *16*(4), 387–400. https://doi.org/10.1017/S0954102004002214

Parkinson, C. L. (2019). A 40-y record reveals gradual Antarctic sea ice increases followed by decreases at rates far exceeding the rates seen in the Arctic. *Proceedings of the National Academy of Sciences*, *116*(29), 14414–14423. https://doi.org/10.1073/pnas.1906556116

Parkinson, C. L., & Cavalieri, D. J. (2012). Antarctic sea ice variability and trends, 1979–2010. *The Cryosphere*, *6*(4), 871–880. https://doi.org/10.5194/tc-6-871-2012

Pegliasco, C., Delepoulle, A., Mason, E., Morrow, R., Faugère, Y., & Dibarboure, G. (2022). META3.1exp: A new global mesoscale eddy trajectory atlas derived from altimetry. *Earth System Science Data*, *14*(3), 1087–1107. https://doi.org/10.5194/essd-14-1087-2022

Rintoul, S. R. (2018). The global influence of localized dynamics in the Southern Ocean. *Nature*, *558*(7709), 209–218. https://doi.org/10.1038/s41586-018-0182-3

Roach, C. J., & Speer, K. (2019). Exchange of water between the Ross Gyre and ACC assessed by Lagrangian particle tracking. *Journal of Geophysical Research: Oceans*, *124*(7), 4631–4643. https://doi.org/10.1029/2018JC014845

Sallée, J. B., Speer, K., & Morrow, R. (2008). Southern Ocean fronts and their variability to climate modes. *Journal of Climate*, *21*(12), 3020–3039. https://doi.org/10.1175/2007JCLI1702.1

Sallée, J. B., Speer, K., & Rintoul, S. (2011). Mean-flow and topography control on surface eddy-mixing in the Southern Ocean. *Journal of Marine Research*, *69*(4), 753–777. https://doi.org/10.1357/002224011799849408

Scambos, T. & Stammerjohn, S. (Eds.) (2018). Antarctica. In *"state of the climate in 2017"*. *Bulletin of the American Meteorological Society* (Vol. 9(8), pp. S175–S190). https://doi.org/10.1175/2018BAMSStateoftheClimate.1

Scambos, T. & Stammerjohn, S. (Eds.) (2019). Antarctica and the Southern Ocean. In *"State of the climate in 2018"*. *Bulletin of the American Meteorological Society* (Vol. 100(9), pp. S169–S188). https://doi.org/10.1175/2019BAMSStateoftheClimate.1

Schlosser, E., Haumann, F. A., & Raphael, M. N. (2018). Atmospheric influences on the anomalous 2016 Antarctic sea ice decay. *The Cryosphere*, *12*(3), 1103–1119. https://doi.org/10.5194/tc-12-1103-2018

Shi, F., Luo, Y., Wu, R., Yang, Q., Chen, R., Wang, C., et al. (2023). Contrasting trends in short-lived and long-lived mesoscale eddies in the Southern Ocean since the 1990s. *Environmental Research Letters*, *18*(3), 034042. https://doi.org/10.1088/1748-9326/acbf6b

Sokolov, S., & Rintoul, S. R. (2009a). Circumpolar structure and distribution of the Antarctic Circumpolar Current fronts: 1. Mean circumpolar paths. *Journal of Geophysical Research*, *114*(C11), C11018. https://doi.org/10.1029/2008jc005108

Sokolov, S., & Rintoul, S. R. (2009b). Circulation structure and distribution of the Antarctic circumpolar current fronts: 2. Variability and relationship to sea surface height. *Journal of Geophysical Research*, *114*(C11), C11019. https://doi.org/10.1029/2008JC005248

Son, S.-W., Gerber, E. P., Perlwitz, J., Polvani, L. M., Gillett, N. P., Seo, K. H., et al. (2010). Impact of stratospheric ozone on southern Hemisphere circulation change: A multimodel assessment. *Journal of Geophysical Research*, *115*, D00M07. https://doi.org/10.1029/2010JD014271

Spreen, G., Kaleschke, L., & Heygster, G. (2008). Sea ice remote sensing using AMSR-E 89 GHz channels. *Journal of Geophysical Research*, *113*(C2), C02S03. https://doi.org/10.1029/2005JC003384

Stammerjohn, S. (Ed.) (2016). Antarctica. In *"state of the climate in 2015". Bulletin of the American Meteorological Society* (Vol. 97(8), pp. S155–S170).

Stammerjohn, S., Massom, R., Rind, D., & Martinson, D. (2012). Regions of rapid sea ice change: An inter-hemispheric seasonal comparison. *Geophysical Research Letters*, *39*(6), L06501. https://doi.org/10.1029/2012GL050874

Stammerjohn, S. & Scambos, T. (Eds.) (2017). *Antarctica In "state of the climate in 2016"*, 98(8), S155–S169. https://doi.org/10.1175/2017BAMSStateoftheClimate.1

Swart, N. C., Ansorge, I. J., & Lutjeharms, J. R. E. (2008). Detailed characterization of a cold Antarctic eddy. *Journal of Geophysical Research*, *113*(C1), C01009. https://doi.org/10.1029/2007JC004190

Taburet, G., Sanchez-Roman, A., Ballarotta, M., Pujol, M.-I., Legeais, J.-F., Fournier, F., et al. (2019). DUACS DT2018: 25 years of reprocessed sea level altimetry products. *Ocean Science*, *15*(5), 1207–1224. https://doi.org/10.5194/os-15-1207-2019

Thompson, A. F., & Sallée, J. B. (2012). Jets and topography: Jet transitions and the impact on transport in the Antarctic circumpolar current. *Journal of Physical Oceanography*, *42*(6), 956–972. https://doi.org/10.1175/JPO-D-11-0135.1

Trani, M., Falco, P., & Zambianchi, E. (2011). Near-surface eddy dynamics in the Southern Ocean. *Polar Research*, *30*(1), 11203. https://doi.org/10.3402/polar.v30i0.11203

Trani, M., Falco, P., Zambianchi, E., & Sallée, J. B. (2014). Aspects of the Antarctic Circumpolar Current dynamics investigated with drifter data. *Progress in Oceanography*, *125*, 1–15. https://doi.org/10.1016/j.pocean.2014.05.001

Turner, J., Comiso, J. C., Marshall, G. J., Lachlan-Cope, T. A., Bracegirdle, T., Maksym, T., et al. (2009). Non-annular atmospheric circulation change induced by stratospheric ozone depletion and its role in the recent increase of Antarctic sea ice extent. *Geophysical Research Letters*, *36*(8), L08502. https://doi.org/10.1029/2009GL037524

Turner, J., Hosking, J. S., Marshall, G. J., Phillips, T., & Bracegirdle, T. J. (2016). Antarctic sea ice increase consistent with intrinsic variability of the Amundsen Sea Low. *Climate Dynamics*, *46*(7–8), 2391–2402. https://doi.org/10.1007/s00382-015-2708-9

Wachter, P., Reiser, F., Friedl, P., & Jacobeit, J. (2021). A new approach to classification of 40 years of Antarctic sea ice concentration data. *International Journal of Climatology*, *41*(1), E2683–E2699. https://doi.org/10.1002/joc.6874

Wang, S., Liu, J., Cheng, X., Kerzenmacher, T., Hu, Y., Hui, F., & Braesicke, P. (2021). How do weakening of the stratospheric polar vortex in the Southern Hemisphere affect regional Antarctic sea ice extent? *Geophysical Research Letters*, *48*(11), e2021GL092582. https://doi.org/10.1029/2021GL092582

Wolff, J. O. (1999). Modelling the Antarctic circumpolar current: Eddy - Dynamics and their Parametrization. *Environmental Modelling & Software*, *14*(4), 317–326. https://doi.org/10.1016/S1364-8152(98)00083-8

Wu, Y., Wang, Z., & Liu, C. (2021). Impacts of changed ice-ocean stress on the North Atlantic Ocean: Role of ocean surface currents. *Frontiers in Marine Science*, *8*, 628892. https://doi.org/10.3389/fmars.2021.628892